Arch. Mech., **66**, 1, pp. 55–65, Warszawa 2014

Brief Note

Existence of zero-group velocity modes in an incompressible plate

T. HUSSAIN, F. AHMAD

Centre for Advanced Mathematics and Physics
National University of Sciences and Technology
Sector H-12, Islamabad, Pakistan
e-mail: htakasar@yahoo.com

Zero-group velocity (ZGV) Lamb modes are studied in an incompressible orthotropic plate. The existence of such modes critically depends on the anisotropy parameter $a = (c_{11} + c_{22} - 2c_{12} - 4c_{66})/c_{66}$. With materials having $a > -1$, none of the modes possesses any ZGV points and every mode has such a point if $a < -1$. Several modes have multiple ZGV points.

Key words: Lamb modes, anisotropy, zero-group velocity points.

1. Introduction

Lamb waves are an important tool for non-destructive testing of materials [1]. This is done by studying the shape of Lamb modes generated by a perturbation of the surface of a mechanical structure, see for example [2]. In a plate, free of defects, the phase speed of each mode, as a function of wave number, exhibits a plateau region and asymptotically approaches a fixed speed [3]. However in the frequency-wave number spectrum, certain modes are anomalous in the sense that, over a narrow frequency interval, the group velocity is directed opposite to the phase velocity. The group velocity vanishes at a point where the dispersion curve undergoes a change in the sign of its slope. Such a point is called a zero-group velocity (ZGV) point. The existence of a ZGV mode was first pointed out by Tolstoy and Usdin [4] in 1957 and these modes have been investigated theoretically and experimentally by several authors [5–12]. Recently Hussain and Ahmad [13] considered ZGV points in the spectrum of Lamb modes in a compressible orthotropic plate. It was found that, in addition to modes with a single ZGV point, a large number of modes exist with multiple such points.

Several problems in elasticity become relatively easy when the material is assumed to be incompressible. This happens because, in this case, a displacement potential function can be introduced [14, 15]. This assumption can be justified in case of materials such as Kraton polymer, thermoplastic elastomers and rubber composites [16]. Rogerson [17] and Ogden and Roxburgh [18] have discussed the dispersion relation for incompressible elastic plate but they did not consider ZGV Lamb modes.

In the present paper, we will consider the effect of the incompressibility constraint on the ZGV modes. Let us define a parameter of elastic anisotropy

$$a = \frac{c_{11} + c_{22} - 2c_{12} - 4c_{66}}{c_{66}}. \tag{1.1}$$

This parameter satisfies the constraint

$$a \geq -4. \tag{1.2}$$

We shall consider symmetric Lamb modes in an incompressible orthotropic plate and show that the numerical value of the anisotropy parameter plays a critical role in the existence, or otherwise, of ZGV points in the spectrum of a material. We shall establish that

(i) No ZGV mode exists if $a > -1$.

(ii) Every mode, with the possible exception of the lowest few modes, is a ZGV mode if $a < -1$.

The above results are established analytically and are borne out by dispersion curves. These curves also exhibit multiple ZGV points for materials with the anisotropy parameter in the range $-4 < a < -3$. Since $a = 0$ for isotropic as well as transversely isotropic materials, it follows that the incompressibility constraint will preclude anomalous modes in such materials.

2. ZGV Lamb modes

The symmetric dispersion relation for the waves propagating in incompressible elastic plates, having thickness $2h$, is given by [17, 18]

$$\frac{\tan(s_1 kh)}{\tan(s_2 kh)} = \frac{s_1(1 - s_2^2)^2}{s_2(1 - s_1^2)^2}, \tag{2.1}$$

where s_1^2 and s_2^2 are roots of the following equation

$$s^4 + \left(a + 2 - \frac{\rho c^2}{c_{66}}\right)s^2 + \left(1 - \frac{\rho c^2}{c_{66}}\right) = 0. \tag{2.2}$$

If we denote dimensionless wave number kh by x and $c/\sqrt{c_{66}/\rho}$ by y, then Eq. (2.1) becomes

$$\frac{\tan(s_1 x)}{\tan(s_2 x)} = \frac{s_1(1 - s_2^2)^2}{s_2(1 - s_1^2)^2}, \tag{2.3}$$

with s_1 and s_2 given by

$$s_1 = \sqrt{\frac{-(a+2-y^2) - \sqrt{(a+2-y^2)^2 - 4(1-y^2)}}{2}}, \tag{2.4}$$

$$s_2 = \sqrt{\frac{-(a+2-y^2) + \sqrt{(a+2-y^2)^2 - 4(1-y^2)}}{2}}. \tag{2.5}$$

The ZGV modes manifest themselves in the $\omega - c$ plane. Let $c_T = \sqrt{c_{66}/\rho}$ denote the shear velocity of the wave and we define the dimensionless variable

$$u = \frac{\omega h}{\sqrt{c_{66}/\rho}} = yx. \tag{2.6}$$

In terms of u and y Eq. (2.3) becomes

$$\frac{\tan(s_1 u/y)}{\tan(s_2 u/y)} = \frac{s_1(1-s_2^2)^2}{s_2(1-s_1^2)^2}. \tag{2.7}$$

Let S_n, $n = 1, 2, \ldots$ denote the n-th mode in the spectrum. To check whether or not a mode is anomalous, we look at the slope of each mode for large as well as small y.

In order to examine slope of the mode S_n we rewrite Eq. (2.7) in the form

$$f(u,y) = \tan(s_1 u/y) s_2 (1-s_1^2)^2 - \tan(s_2 u/y) s_1 (1-s_2^2)^2 = 0. \tag{2.8}$$

For large y,

$$s_1 \simeq i, \tag{2.9}$$

$$s_2 \simeq y\left(1 - \frac{a+1}{2y^2}\right), \tag{2.10}$$

and Eq. (2.8) becomes

$$\tan\left(u_n\left(1 - \frac{a+1}{2y^2}\right)\right) \simeq 0. \tag{2.11}$$

We will determine the slope dy/du by using the following formula

$$\frac{dy}{du} = -\frac{\partial f/\partial u}{\partial f/\partial y}. \tag{2.12}$$

The partial derivatives can be approximated, for large y, as follows

$$\frac{\partial f}{\partial u} \simeq i(4 - y^4), \tag{2.13}$$

$$\frac{\partial f}{\partial y} \simeq -i u_n (a+1) y. \tag{2.14}$$

Using these expressions we have, for large y,

$$\frac{dy}{du} \simeq -\frac{y^3}{u_n(a+1)}, \quad n = 1, 2, \dots . \tag{2.15}$$

If $a+1>0$, then

$$\frac{dy}{du} < 0 \qquad \text{for } S_n,\ n \geq 1. \tag{2.16}$$

For $a+1<0$, we have

$$\frac{dy}{du} > 0 \qquad \text{for } S_n,\ n \geq 1. \tag{2.17}$$

Now we will estimate the slope when y approaches the line $y=1$ from above. First consider the case when $a+1<0$. Let $b=-(a+1)>0$ and $y^2=1+\epsilon^2$, where ϵ is a small positive number. Then

$$\begin{aligned} s_1^2 &= \frac{b+\epsilon^2-\sqrt{(b+\epsilon^2)^2+4\epsilon^2}}{2}, \\ s_1^2 &\simeq \frac{1}{2}\left[b+\epsilon^2-b\sqrt{\left(1+\epsilon^2\frac{2b+4}{b^2}\right)}\right], \\ s_1^2 &\simeq -\frac{\epsilon^2}{b}, \end{aligned} \tag{2.18}$$

where we have ignored terms of order ϵ^3 or higher. Also

$$s_2^2 \simeq b. \tag{2.19}$$

With $s_1=\frac{i\epsilon}{\sqrt{b}}$, $s_2=\sqrt{b}$ Eq. (2.8) becomes

$$\frac{\tanh(\frac{\epsilon u}{\sqrt{b}})}{\tan(\sqrt{b}u)} = \frac{\epsilon(1-b)^2}{b(1+\frac{\epsilon^2}{b})^2}, \tag{2.20}$$

or

$$\tanh\left(\frac{\epsilon u}{\sqrt{b}}\right) \simeq \frac{(1-b)^2}{b}\tan(\sqrt{b}u)\epsilon. \tag{2.21}$$

The partial derivatives can be approximated, in this case, as follows

$$\frac{\partial f}{\partial u} \simeq -i\epsilon\sqrt{b}\left(\frac{(1-b)^2}{\sqrt{b}}+\frac{u^2\sqrt{b}}{(1-b)^2}-\frac{1}{\sqrt{b}}\right), \tag{2.22}$$

$$\begin{aligned} \frac{\partial f}{\partial y} \simeq &\ \frac{i\epsilon u}{b^2(1-b)^2} \\ &\times[(1+b)(1-b)^2-(1-b)^4(1+b-b^2)+8b(1-b)-b(a+3)u^2]. \end{aligned} \tag{2.23}$$

Using these expressions we have, for $y \to 1^+$,

$$\frac{dy}{du} \simeq \frac{b^3[(b-2)(1-b)^2+u_n^2]}{u_n[(1+b)(1-b)^2-(1-b)^4(1+b-b^2)+8b(1-b)-b(a+3)u_n^2]}, \tag{2.24}$$

for $n = 1, 2, \ldots$. From Eq. (2.24), it is clear that when $a + 3 > 0$ and $y \to 1^+$, $dy/du < 0$ for sufficiently large u_n.

Next let $1 + a > 0$. In this case

$$s_1^2 \simeq -(a + 1), \tag{2.25}$$

$$s_2^2 \simeq \frac{\epsilon^2}{a + 1}. \tag{2.26}$$

Equation (2.8) becomes

$$\frac{\tanh(\sqrt{a+1}u)}{\tan(\frac{\epsilon}{\sqrt{a+1}}u)} \simeq \frac{a+1}{\epsilon} \frac{(1 - \frac{\epsilon^2}{1+a})^2}{(a + 2)^2}. \tag{2.27}$$

The above equation was considered by AHMAD [3]. All modes, except S_0, approach the line $y = 1$ with negative slope.

Thus we have established that, in case of materials with $a+1 > 0$, the modes maintain their negative slope from their inception when $y \to \infty$ to the eventual non-oscillation limit when $y \to 1^+$. These modes are free of anomalous behavior and do not possess any ZGV points.

However for materials with $a + 1 < 0$ and $a + 3 > 0$ i. e. $-3 < a < -1$, Eq. (2.15) indicates that the slope is positive for large y while Eq. (2.24) shows that, for sufficiently large u_n, the slope becomes negative when $y \to 1^+$. This change in the sign of slope leads to at least one ZGV point for each mode in the spectrum, with the possible exception of the first few modes.

The case $-4 < a < -3$ still needs to be sorted out. For this purpose, we calculate the slope for that value of y, say y_0, at which the lowest mode, S_0, is born. To find y_0, let $u \to 0$ in Eq. (2.7). This leads to

$$(1 - s_1^2)^2 = (1 - s_2^2)^2, \tag{2.28}$$

or

$$s_1^2 + s_2^2 = 2, \tag{2.29}$$

is the only acceptable solution of Eq. (2.7) when $-4 < a < -3$. From Eq. (2.2),

$$s_1^2 + s_2^2 = -(a + 2 - y^2), \tag{2.30}$$

hence

$$y_0^2 = a + 4, \tag{2.31}$$

or

$$y_0 = \sqrt{a+4}. \tag{2.32}$$

For the range of a under consideration, $0 < y_0 < 1$. The lowest mode starts above or below the line $y = 1$ according as $a + 3$ is positive or negative.

The derivative is given by the following expression:

$$\frac{dy}{du}\Big|_{y=y_0} = \frac{4s_1^2(a+4)s_2\sin^2(s_2u_n/y_0)}{2u_ns_2(a+2)\sqrt{a+4}\cos^2(s_2u_n/y_0) + (a+4)(3a+10)\sin(s_2u_n/y_0)}, \tag{2.33}$$

for $n = 1, 2, \ldots$.

When $y = y_0$, s_1, s_2 respectively are found from Eqs (2.4) and (2.5) as

$$s_1 = \sqrt{1-y_0}, \qquad s_2 = \sqrt{1+y_0}.$$

Since y_0 does not equal zero or 1, vanishing of $\cos(s_2u_n/y_0)$ is ruled out by Eq. (2.7). Also $a + 2 < 0$, hence

$$\left.\frac{dy}{du}\right|_{y=y_0} < 0, \tag{2.34}$$

for sufficiently large u_n. Thus modes will undergo a change of sign and each of them will possess a ZGV point.

We have established the result that, with the possible exception of first few modes, no mode will be anomalous if $a+1 > 0$ and every mode will be anomalous if $a + 1 < 0$.

Table 1 shows values of anisotropy parameter a for a few orthotropic materials.

Table 1. Value of the anisotropy parameter

Material	Value of anisotropy parameter a	Source
Iodic acid	−0.4620	20
Barium sodium niobate	−0.3421	20
Lead chloride	4.5625	21
Gallium	−1.1166	21
Cadmium formate	−2.4894	21
Forsterite	0.8952	21
Rubidium sulfate	0.4043	21
Calcium formate	−3.1489	21

We have plotted the dispersion curves, using the technique of Honarvar *et al.* [19].

Figure 1 exhibits the dispersion curves for barium sodium niobate which has $a = -0.3421$.

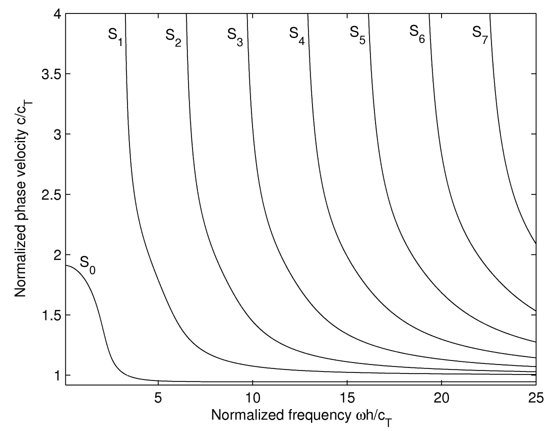

Fig. 1. Symmetric Lamb modes for an incompressible orthotropic barium sodium niobate material with $a = -0.3421$ in (ω, c) plane. No mode is anomalous.

Figure 2 depicts the anomalous modes S_2, S_3, S_4, S_5 for the spectrum of calcium formate which has $a = -3.1489$.

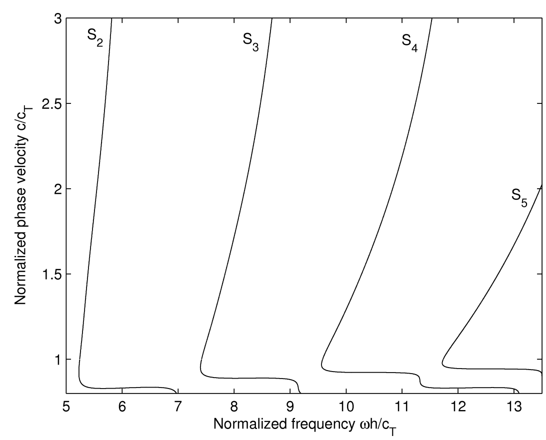

Fig. 2. Symmetric Lamb modes for an incompressible orthotropic calcium formate material with $a = -3.1489$ in (ω, c) plane. All modes are anomalous except S_0 and S_1.

The Lamb modes, having three ZGV points, S_6, S_7, S_8, S_9, S_{10} for calcium formate are plotted in Figure 3.

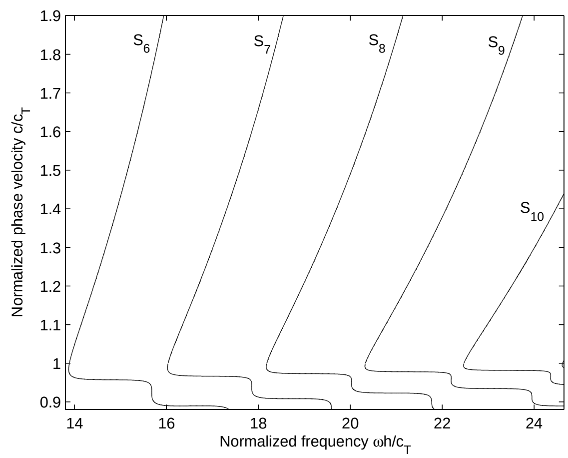

Fig. 3. Symmetric Lamb modes for an incompressible orthotropic calcium formate material with $a = -3.1489$ in (ω, c) plane.

In Figure 4, we have plotted first seven Lamb modes for calcium formate in (k, ω) plane.

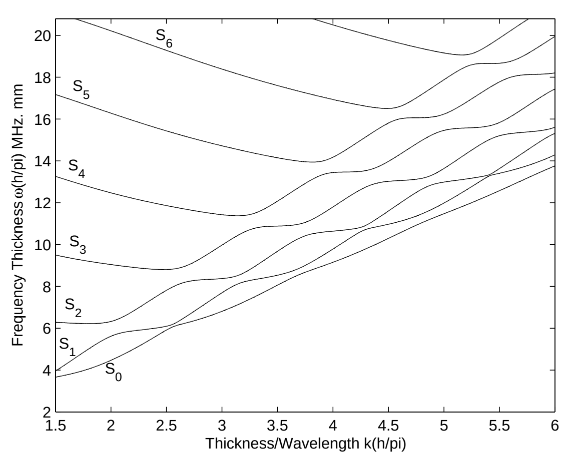

Fig. 4. First 7 symmetric Lamb mode for an incompressible orthotropic calcium formate material with $a = -3.1489$ in (k, ω) plane.

One can easily observe that all modes, except S_0 and S_1, have at least one ZGV point, but S_6 is the first mode which has three ZGV points. The modes S_4 and S_5 also *seem* to have multiple ZGV points but a closer inspection does not bear this out. This becomes clear in Fig. 5, where we have focused on that part of S_4 where the second and third ZGV points appear to exist. However a similar

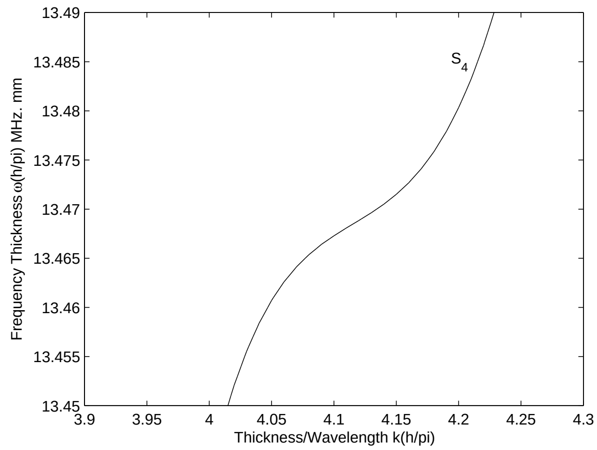

FIG. 5. The S_4 symmetric Lamb mode for an incompressible orthotropic calcium formate material in (k, ω) plane.

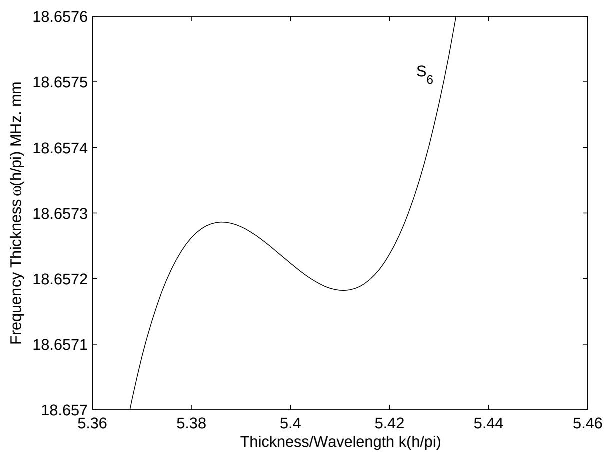

FIG. 6. The S_6 symmetric Lamb mode with second and third ZGV points for an incompressible orthotropic calcium formate material in (k, ω) plane.

focus on the corresponding domain of S_6 in Fig. 6 clearly indicates the existence of the second and third ZGV points.

Acknowledgements

The authors are grateful to a referee for helpful comments which led to improvement of the paper. The first author is thankful to the National University of

Sciences and Technology for financial support. The second author acknowledges financial support of the Higher Education Commission of Pakistan.

References

1. W.J. Staszewski, B.C. Lee, R. Traynor, *Fatigue detection in metallic structures with Lamb waves and 3D laser vibrometry*, Measurement Science and Technology, **18**, 727–739, 2007.

2. N. Ryden, C.B. Park, P. Ulriksen, R.D. Miller, *Lamb wave analysis for nondestructive testing of concrete plate structures*, Proceedings of the Symposium on the Application of Geophysics to Engineering and Environmental Problems (SAGEEP), San Antonio, TX, April 6–10, INF03, 2003.

3. F. Ahmad, *Shape of dispersion curves in the Rayleigh-Lamb spectrum*, Arch. Mech., **56**, 157–165, 2004.

4. I. Tolstoy, E. Usdin, *Wave propagation in elastic plates: low and high mode dispersion*, J. Acoust. Soc. Am., **29**, 37–42, 1957.

5. K. Negishi, *Existence of negative group velocities in Lamb waves*, Jpn. J. Appl. Phys., Suppl. **26**, (1), 171–173, 1987.

6. M.F. Werby, H. Uberall, *The analysis and interpretation of some special properties of higher order symmetric Lamb waves: The case for plates*, J. Acoust. Soc. Am., **111**, 2686–2691, 2002.

7. A.H. Meitzler, *Backward wave transmission of stress pulses in elastic cylinders and plates*, J. Acoust. Soc. Am., **38**, 835–842, 1965.

8. K. Nishimiya, K. Mizutani, N. Wakatsuki, K. Yamamoto, *Determination of condition for fastest NGV of Lamb-type waves under each density ratio of solid and liquid layers*, Acoustics 08, Paris, P. 3613.

9. S.D. Holland, D.E. Chimenti, *Air-coupled acoustic imaging with zero-group-velocity Lamb modes*, Appl. Phys. Lett., **83**, 2704–2706, 2003.

10. C. Prada, O. Balogun, T.W. Murray, *Laser-based ultrasonic generation and detection of zero-group velocity Lamb waves in thin plates*, Appl. Phys. Lett., **87**, 194109-1-194109-3, 2005.

11. C. Prada, D. Clorennce, T.W. Murray, D. Royer, *Influence of the anisotropy on zero-group velocity Lamb modes*, J. Acoust. Soc. Am., **126**, 620–625, 2009.

12. C. Prada, D. Clorennec, D. Royer, *Local vibration of an elastic plate and zero-group velocity Lamb modes*, J. Acoust. Soc. Am., **124**, 203–212, 2008.

13. T. Hussain, F. Ahmad, *Lamb modes with multiple zero-group velocity points in an orthotropic plate*, J. Acoust. Soc. Am., **32**, 641–645, 2012.

14. S. Nair, D.A. Sotiropoulos, *Elastic waves in orthotropic incompressible materials and reflection from an interface*, J. Acoust. Soc. Am., **102**, 102–109, 1997.

15. R.W. Ogden, P.C. Vinh, *On Rayleigh waves in incompressible orthotropic elastic solids*, J. Acoust. Soc. Am., **115**, 530–533, 2004.

16. S. NAIR, D.A. SOTIROPOULOS, *Interfacial waves in incompressible monoclinic materials with an interlayer*, Mech. Mater. **31**, 225–233, 1999.

17. G.A. ROGERSON, *Some asymptotic expansions of the dispersion relation for an incompressible elastic plate*, Int. J. Solids Struct., **34**, 2785–2802, 1997.

18. R.W. OGDEN, D.G. ROXBURGH, *The effect of pre-stressed on the vibration and stability of elastic plates*, Int. J. Engng Sci., **31**, 1611–1639, 1993.

19. F. HONARVAR, E. ENJILELA, A.N. SINCLAIR, *An alternative method for plotting dispersion curves*, Ultrasonics, **49**, 15–18, 2009.

20. D. ROYER, E. DIEULESAINT, *Elastic Waves in Solids 1 Free and Guided Propagation*, Chapter 3, Springer, Berlin, 2000.

21. K.H. HELLWEGE, A.M. HELLWEGE, *LANDOLT-BORNSTEIN Numerical Data and Functional Relationships in Science and Technology*, Chapter 1, Springer, Berlin, 1979.

Received May 2, 2013; revised version September 2, 2013.